Analytical Study of Nonlinear Controls Applied to Wind Energy Conversion Systems Using a DFIG

Abdelmajid Berdai, Moussa Reddak, Abdelaziz Belfqih, Boukherouaa Jamal, Faissal El Mariami and Abdelhamid Hmidat

Abstract Variable-speed wind energy conversion systems (WECSs) have become increasingly important in recent years as they enable obtainment of maximal output power in the fields of the low and average wind speeds. In this study, we focus on WECS using doubly-fed induction generators (DFIGs) and present models for the turbine and doubly-fed induction generator. The main objective is to study two types of nonlinear controls; sliding mode and backstepping used for control of the grid-side converter will be also studied and analyzed. Matlab / Simulink simulation results are included.

1 Introduction

Increases in energy demand are posing an ever greater challenge across the world. Rapid growth of industrial activity in developed countries and in investments by companies in countries that ensure lower production costs has led to spiraling increases in energy demand worldwide –increases expressed in rising prices for oil, which remains the leading energy source. World oil reserves continue to diminish and in future years there will not be enough to meet demand. The earth's climate is deteriorating and natural sources of water are becoming scarcer. Nuclear energy is not available to everybody for political, technological or financial reasons; its installation is expensive and it can be dangerous ecologically. Use of such conventional sources is therefore either limited or not encouraged for environmental reasons. And so the world is turning to renewable sources – sun, wind, underwater currents etc. – to produce electricity [1].

A. Berdai(✉) · M. Reddak · A. Belfqih · B. Jamal · F. El Mariami · A. Hmidat
ESE Research Group, Department of Electrical Engineering, National School of Electricity and Mechanics ENSEM, University Hassan II, Casablanca, Morocco
e-mail: {a.berdai,moussa.reddak}@gmail.com, a-belfqih@hotmail.com, {j.boukherouaa,f_elmariami,a.hmidat}@yahoo.fr

© Springer Science+Business Media Singapore 2016

E. Sabir et al. (eds.), *The International Symposium on Ubiquitous Networking*,
Lecture Notes in Electrical Engineering 366,
DOI: 10.1007/978-981-287-990-5_37

At present, variable-speed wind systems based on the doubly fed induction generator (DFIG) are the systems most commonly used in land wind farms. Their implementation in renewable energy conversion systems has increased dramatically due to their many advantages, which include low cost, small size, and the ability to produce maximum power under various wind and rotational speeds. The DFIG enables functioning on a range of speeds of ± 30 % around the simultaneous speed, so ensuring reduced sizing of the static converters, as these latter are connected between the rotor winding [2].

Growing interest is being shown in this machine, largely due to the degree of freedom it provides, owing to its rotor's accessibility and the consequent possibility of supplying it via a converter on the stator side and rotor side alike, as well as extending the speed range (sub-synchronous, synchronous and above-synchronous) [3].

2 Modeling of DFIG System

2.1 Model of the Wind Turbine

If the kinetic energy of a mass of air moving at speed v could be fully recovered using a device with surface A, located perpendicular to wind speed direction, instantaneous power would be [4]:

$$P_e = \frac{1}{2}\rho A v^3. \tag{1}$$

In reality, however, a wind turbine extracts a power P lower than available power Pe, as a result of the non-null speed of air masses behind the aero-engine. Wind energy conversion aptitude is given by the power coefficient Cp, defined by the relationship:

$$C_p = \frac{P}{P_e}\,; C_p < 1. \tag{2}$$

$$\lambda = \frac{R\Omega_t}{v}. \tag{3}$$

With $A = \pi R^2$

$$P_t = \frac{\rho \pi R^2 v^3}{2} C_p. \tag{4}$$

2.2 Model of DFIG

In complex notation, the DFIG equations are derived from the Park model expressed in a reference frame d-q rotating at synchronous speed ωs. The electrical energy conversion system is described by the induction machine equations shown in [5]:

$$\begin{cases} V_{ds} = R_s I_{ds} + \frac{d\varphi_{ds}}{dt} - \omega_s \varphi_{qs} \\ V_{qs} = R_s I_{qs} + \frac{d\varphi_{qs}}{dt} + \omega_s \varphi_{qs} \\ V_{dr} = R_r I_{dr} + \frac{d\varphi_{dr}}{dt} - (\omega_s - \omega_r)\varphi_{qr} \\ V_{qr} = R_r I_{qr} + \frac{d\varphi_{qr}}{dt} + (\omega_s - \omega_r)\varphi_{rs} \\ C_{em} = P(\varphi_{sd} i_{sq} + \varphi_{sq} i_{sd}) \end{cases} \quad (5)$$

The expressions of stator and rotor fluxes in the dq-axis system:

$$\begin{cases} \varphi_{ds} = L_s I_{ds} + M I_{dr} \\ \varphi_{qs} = L_s I_{qs} + M I_{qr} \\ \varphi_{dr} = L_s I_{dr} + M I_{ds} \\ \varphi_{qr} = L_s I_{qr} + M I_{qs} \end{cases} \quad (6)$$

Active and reactive powers exchanged between stator and grid may be expressed as follows:

$$\begin{cases} P_s = V_{ds} I_{ds} + V_{qs} I_{qs} \\ Q_s = V_{qs} I_{ds} - V_{ds} I_{qs} \end{cases} \quad (7)$$

We use the simplification of oriented flux equations:

$$\begin{cases} \varphi_{ds} = L_s I_{ds} + M I_{dr} = \varphi_s \\ \varphi_{qs} = L_s I_{qs} + M I_{qr} = 0 \end{cases} \quad (8)$$

3 Architecture of Control System

The architecture of the control system is presented in Figure 1. It is based on the three-phase model of the channel of electro-mechanical wind-system conversion.

As shown in Figure 1, three detailed controls are then necessary to insure functioning of the wind turbine:

- Control of extraction of maximum wind power via a control known as "MPPT" (Maximum Power Point Tracking).
- Control of the machine-side converter (RSC) by controlling the electromagnetic torque and the DFIG's reactive stator power.
- Control of the GSC by controlling the continuous bus voltage and the active and reactive powers exchanged with the grid.

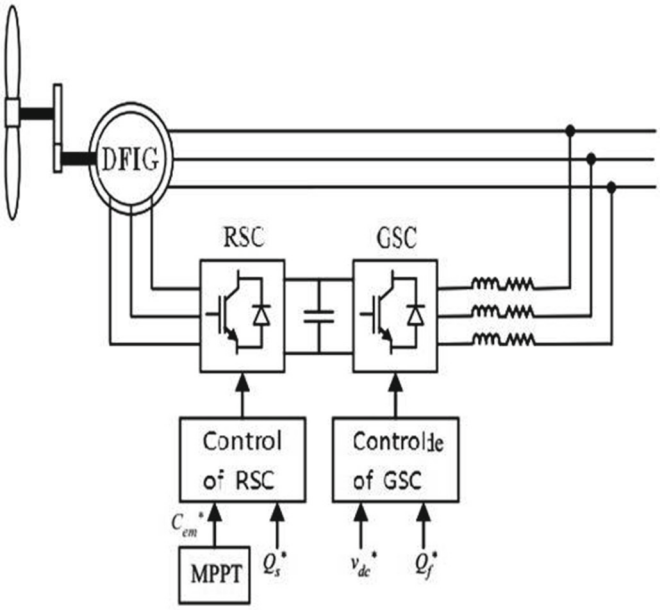

Fig. 1 Architecture of the wind energy control system

3.1 MPPT Control Strategy

Computation of Reference Torque [6]

In this case, system control has to impose a reference torque so as to enable the DFIG to turn at an adjustable speed to ensure an optimal functioning point in terms of maximum power extraction. In this context, the ratio of the speed of wind turbine λ must be maintained at its optimal value ($\lambda = \lambda_{opt}$) on a set range of wind speeds, so maintaining the power coefficient at its maximal value ($C_p = C_{p\_max}$). In this case, the aerodynamic torque may be expressed as:

$$C_{aero} = \frac{1}{2\Omega_t} C_{p\_max} \rho S v^3 \tag{9}$$

$$C_{g\_ref} = \frac{1}{G} C_{aero} \tag{10}$$

Assuming that the angle of orientation of blades ß is constant, wind speed can be estimated as follows:

$$v = \frac{R\hat{\Omega}_t}{\lambda_{opt}} \tag{11}$$

The electromagnetic reference torque may therefore be expressed as follows:

$$C_{em}^* = \frac{1}{2\Omega_t G} C_{p\_max} \rho S v^3 \tag{12}$$

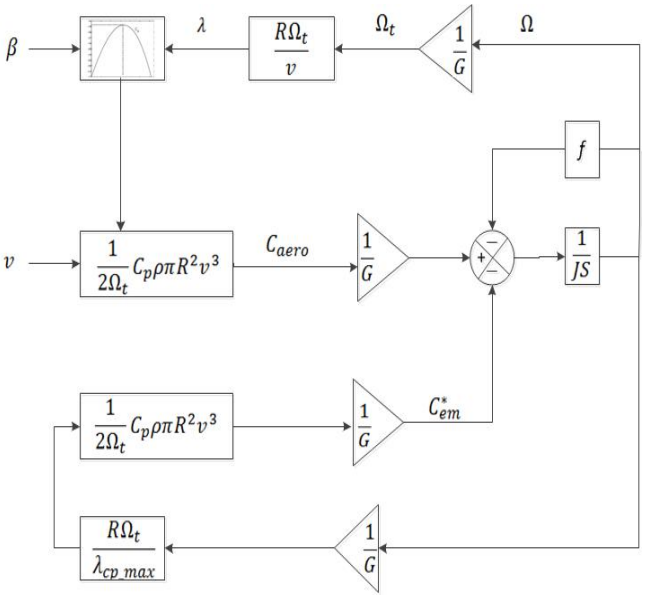

Fig. 2 MPPT control strategy

3.2 Rotor-Side Converter Control

Electromagnetic torque and stator reactive power control will be obtained by controlling the DFIG dq rotor currents.

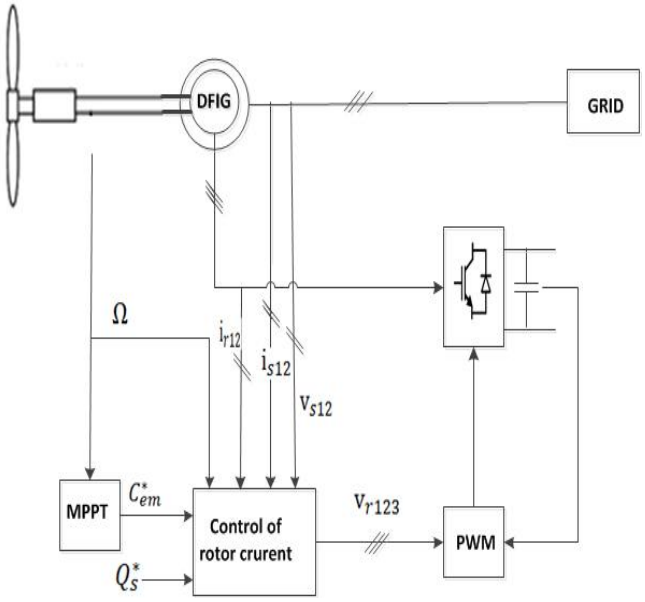

Fig. 3 Rotor-side converter control

3.3 Generation of Rotor Current References

Knowledge of the stator flux is required for generation of the dq axes reference rotor currents (see Figure 3). In our study, the electricity grid is assumed to be stable and the selected dq reference point is connected to the rotating stator field: thus, d axis stator flow may be estimated in open-loop from measurements of stator and d-axis rotor currents:

$$\varphi_{sd-est} = L_s.i_{sd} + M.i_{rd} \tag{13}$$

By estimating the stator flux, we generate the dq axis rotor reference currents. As the electromagnetic torque is proportional to q axis rotor current (according to equation 5), we can establish a relationship between current irq* and electromagnetic torque Cem* from the control MPPT block, by:

$$i_{rq}^{*} = -\frac{L_s}{p.M.\varphi_{sd-est}} C_{em}^{*} \tag{14}$$

Expression of current ird* according to reactive power Qs* is established by:

$$i_{rd}^{*} = \frac{\varphi_{sd-est}}{M} - \frac{L_s}{M.v_{sq}} Q_s^{*} \tag{15}$$

3.4 Grid-Side Converter Control [7][8]

The grid-side converter (GSC) is connected between the continuous bus and the grid via an RL filter. This converter has two roles: to maintain the bus' constant

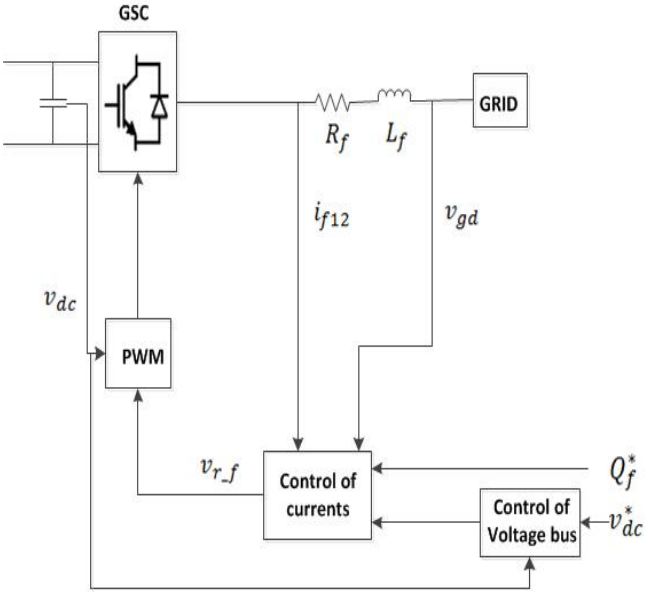

Fig. 4 .Grid-side converter control principle

continuous voltage whatever the amplitude and direction of the MADA rotor power flow and to maintain a power factor equal to 1 at the point of connection with the grid. Figure 4 describes the GSC control, which has a dual function: - Control of currents circulating in filter RL, Control of continuous bus' voltage.

3.5 Control of Filter Currents

The dynamic model of the grid-side inverter side in the reference frame rotating synchronously with the grid voltage vector is:

$$\begin{cases} L_f \frac{di_{d-f}}{dt} = v_{rd} - R_f i_{d-f} + \omega L_f i_{q-f} \\ L_f \frac{di_{q-f}}{dt} = v_{rq} - R_f i_{q-f} - \omega L_f i_{d-f} + Vgd \end{cases} \tag{16}$$

$$\begin{cases} P_f = \frac{3}{2}(V_{gd} i_{d-f} + V_{gq} i_{q-f}) \\ Q_f = \frac{3}{2}(V_{gd} i_{d-f} - V_{gq} i_{q-f}) \end{cases} \tag{17}$$

Where vrd and vrq are the converter d-axis and q-axis voltage components; Vgd is the grid voltage component in the d-axis; idf and iqf are the grid's d-axis current and q-axis current; Lf is the filter inductance; Rf is the filter resistance, and x is the network angular frequency.

$$\begin{cases} P_f = \frac{3}{2} V_{gd} i_{d-f} \\ Q_f = -\frac{3}{2} V_{gd} i_{q-f} \end{cases} \tag{18}$$

By ignoring losses in resistance Rf of the RL filter and taking account of the orientation of the dq reference voltage linked to d-axis (vgq = 0), the equations become:

$$\begin{cases} i_{dr-f} = \frac{2P_f^*}{3V_{gd}} \\ i_{qr-f} = -\frac{2Q_f^*}{3V_{gd}} \end{cases} \tag{19}$$

Accordingly, active and reactive power control can be achieved by controlling direct and quadrature current components respectively. Moreover, the basic aim of the grid-side converter control is to produce no reactive power and to transfer all active power produced by the DFIG to the grid.

Where id_{rf} and iq_{rf} are the desired values of d-axis current and q-axis current respectively. In addition, q-axis currentiq_{rf}, is directly given from the outside of the controller and it sets to zero to achieve unity power factor control.

4 Examples of Nonlinear Control

4.1 Sliding Mode Control

In order to regulate the current components iq and id to their references, the sliding surfaces must be defined as follows:

$$\begin{cases} S_{d-f} = i_{dr-f} - i_{d-f} \\ S_{q-f} = i_{qr-f} - i_{q-f} \end{cases} \tag{20}$$

It follows that:

$$\begin{cases} \frac{dS_{d-f}}{dt} = \frac{di_{dr-f}}{dt} - \frac{di_{d-f}}{dt} = \frac{di_{dr-f}}{dt} - \frac{1}{L_f}(v_{rd} - R_f i_{d-f} + \omega L_f i_{q-f}) \\ \frac{dS_{q-f}}{dt} = \frac{di_{qr-f}}{dt} - \frac{di_{q-f}}{dt} = \frac{di_{qr-f}}{dt} - \frac{1}{L_f}(v_{rq} - R_f i_{q-f} - \omega L_f i_{d-f} - Vgd) \end{cases} \tag{21}$$

When the sliding mode occurs on the sliding surfaces:

$$\begin{cases} S_{d-f} = \frac{dS_{d-f}}{dt} = 0 \\ S_{q-f} = \frac{dS_{q-f}}{dt} = 0 \end{cases} \tag{22}$$

Combining (21) and (22), controls of d axis and q axis voltages are defined by:

$$\begin{cases} v_{rd}^{eq} = L_f \frac{di_{d-f}}{dt} + R_f i_{d-f} - \omega L_f i_{q-f} \\ v_{rq}^{eq} = L_f \frac{di_{q-f}}{dt} + R_f i_{q-f} + \omega L_f i_{d-f} + Vgd \end{cases} \tag{23}$$

Expression of the sliding terms is given by:

$$\begin{cases} V_{dr-n} = L_f K_{d-f} sgn(S_{d-f}) \\ V_{qr-n} = L_f K_{q-f} sgn(S_{d-f}) \end{cases} \tag{24}$$

As a result, the control voltages of q axis and d axis are defined by:

$$V_{r-f} = V^{eq} + V_{r-n}$$
$$\begin{cases} v_{dr-f} = L_f \frac{di_{d-f}}{dt} + R_f i_{d-f} - \omega L_f i_{q-f} + L_f K_d sng(S_{d-f}) \\ v_{qr-f} = L_f \frac{di_{q-f}}{dt} + R_f i_{q-f} + \omega L_f i_{d-f} + Vgd + L_f K_q sng(S_{q-f}) \end{cases} \tag{25}$$

4.2 Backstepping Control

The basic idea behind Backstepping design is the use of so-called “virtual control” to systematically decompose a complex nonlinear control design problem into

simpler, smaller ones. In general terms, Backstepping design is divided into a series of steps, each essentially dealing with an easier, single-input-single-output design problem, and each providing a reference for the next design step. Overall stability and performance are achieved by a Lyapunov function for the whole system [8].

In the first step, the system must follow a given trajectory for each output variable. To do so, two functions are defined, where i_{d-f} and i_{q-f} are the dq-axis current references respectively. The rotor and stator currents tracking error are defined by [9]:

$$\begin{cases} e_1 = i_{d-f} - i_{dr-f} \\ e_2 = i_{q-f} - i_{qr-f} \end{cases} \tag{26}$$

The derivative of Eq. (13) gives:

$$\begin{cases} \dot{e_1} = \dot{\imath_{d-f}} - \dot{\imath_{dr-f}} \\ \dot{e_2} = \dot{\imath_{q-f}} - \dot{\imath_{qr-f}} \end{cases} \tag{27}$$

By replacing the equation, we obtain the following expressions;

$$\begin{cases} \dot{e_1} = \dot{\imath_{d-f}} - \frac{1}{L_f}(v_{rd} - R_f i_{d-f} + \omega L_f i_{q-f}) \\ \dot{e_2} = \dot{\imath_{q-f}} - \frac{1}{L_f}(v_{rq} - R_f i_{q-f} - \omega L_f i_{d-f} - Vgd) \end{cases} \tag{28}$$

To improve control performances in terms of stability, we use the following Lyaponov functon:

$$V = \frac{1}{2}(e_1^2 + e_2^2) \tag{29}$$

Using eq (28), the derivative of eq. (29) is written as follows:

$$\dot{V} = \dot{e_1} e_1 + \dot{e_2} e_2$$

$$e_1\left(\frac{1}{L_f}\left(v_{dr-f} - R_f i_{d-f} + \omega L_f i_{q-f}\right) + K_1 e_1\right)$$

$$+ e_2.\left(\frac{1}{L_f}\left(v_{qr-f} - R_f i_{q-f} - \omega L_f i_{d-f} - Vgd + K_2 e_2\right) - K_1 e_1^2\right.$$

$$\left. - K_2 e_2^2\right.$$

The derivative of the complete Lyapunov function eq. (26) can be negative definite if the quantities between parentheses in eq. (26), are chosen equal to zero.

$$\begin{cases} \frac{1}{L_f}\left(v_{dr-f} - R_f i_{d-f} + \omega L_f i_{q-f}\right) + K_1 e_1 = 0 \\ \frac{1}{L_f}\left(v_{qr-f} - R_f i_{q-f} - \omega L_f i_{d-f} - Vgd + K_2 e_2\right) = 0 \end{cases}$$

$$\dot{V} = -K_1 e_1^2 - K_2 e_2^2 \leq 0$$

Rotor voltages may then be deduced as follows:

$$\begin{cases} v_{dr-f} = R_f i_{d-f} - \omega L_f i_{q-f} - K_1 e_1 \\ v_{qr-f} = R_f i_{q-f} + \omega L_f i_{d-f} + Vgd - K_2 e_2 \end{cases}$$

5 Simulation Results

5.1 Sliding Mode Control

As we mentioned in Part III, control of active power is achieved by controlling direct component Id of the rotor current, and control of reactive power is achieved by controlling the component in quadrature Iq.

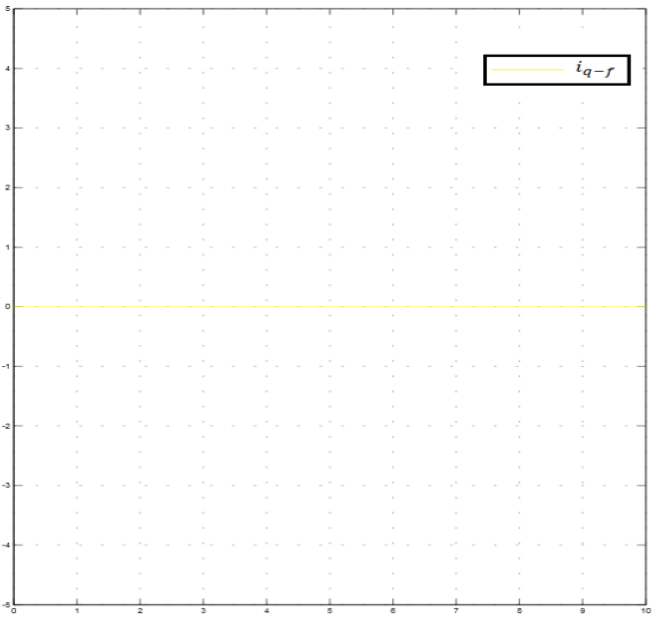

Fig. 5 Iq current response

The Figure 5 presents the temporal evolution of the reactive power. The wind system works in Unitarian power factor because the reactive power of reference Qf* is imposed equal to zero.

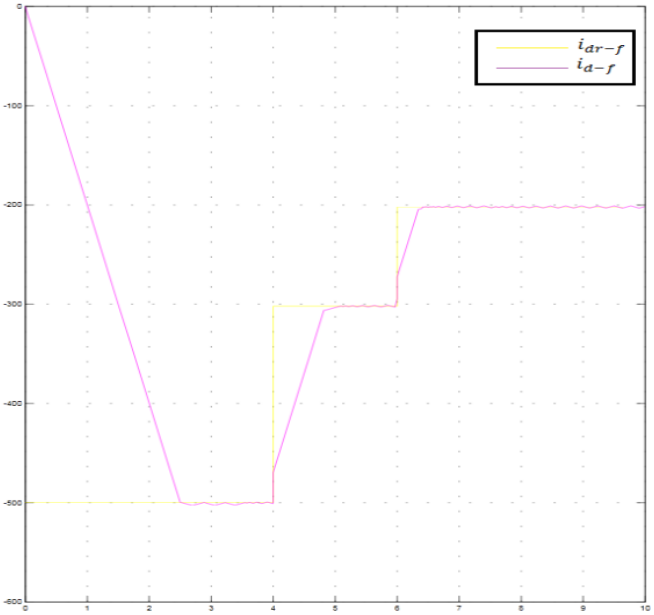

Fig. 6 Control of Id component

5.2 Backstepping Control

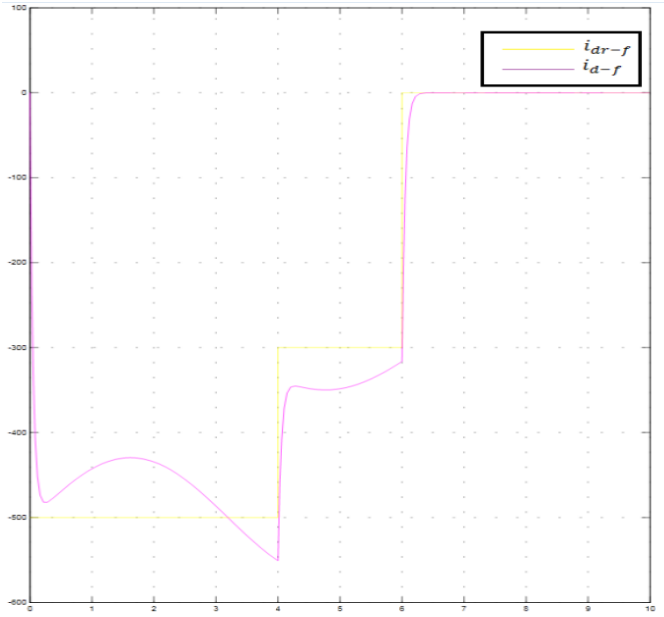

Fig. 7 Control of active power by Id component current

The Figures 6 and 7 shows the regulation of the active power that controlled by the component Id. The power imposed varies in three levels. Which mean that the active power is dependent at the request of the consumers.

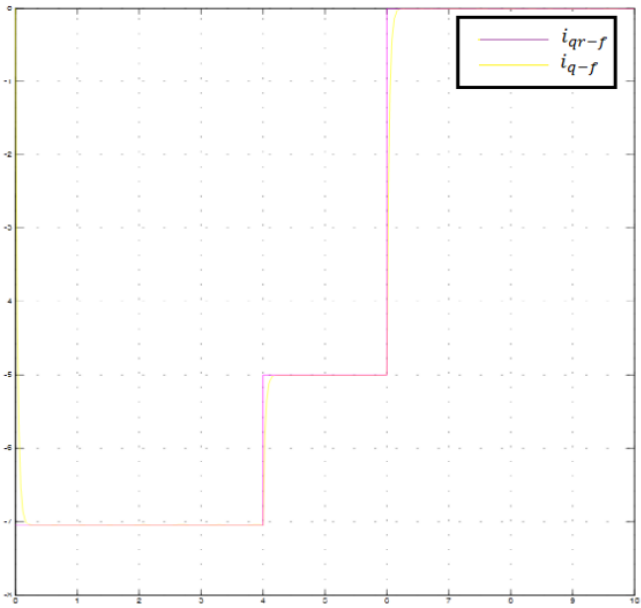

Fig. 8 Control of reactive power by Iq component current

Between times t = 4 and t = 6, we have changed the reactive power reference, which means that to the reference changes on the rotor current ird (Figure) 8). We notice that the time of response of the system is satisfactory and that the reactive power supplied by the wind system is regulated well in its reference value.

The parameters of the grid and the controllers (Backstepping and sliding mode) are given by the following table.

Parameter of the grid	Parameter of backstepping control	Parameter of sliding mode control
L_f =0.22	K_1 =20	K_1 =200
R_f =1.3	K_2 =30	K_1 =6

6 Analytical Study

6.1 The 'Chattering' Phenomenon

The control technique described in the sliding mode control part brings about unwanted behavior in the closed-loop system. However, ideally, it requires an

infinite switching of actuators. Such oscillation close to the surface is known as 'chattering'. Figure (10) shows the effect of chattering in convergence of the system. Chattering is not desirable as it induces high frequency dynamics in the system, increasing energy consumption which can damage the actuators [10].

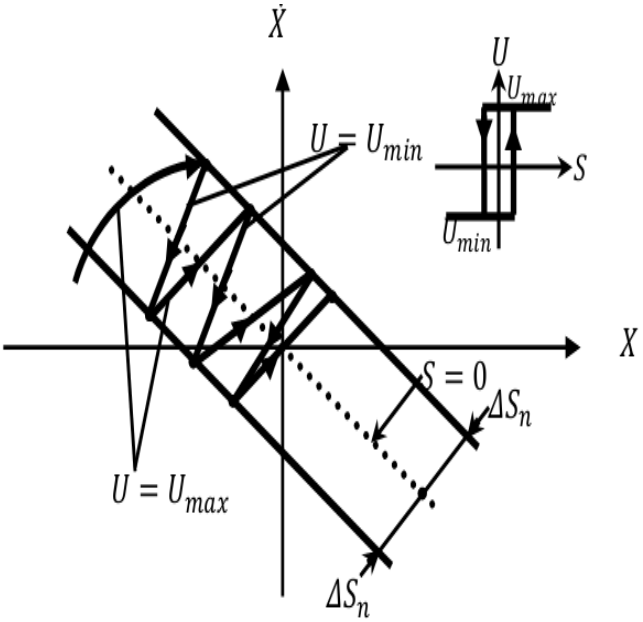

Fig. 9 Demonstration of the 'chattering' phenomenon

Chattering is the main disadvantage of sliding mode control. Numerous studies have been undertaken with the aim of reducing or eliminating the problem – for example, proposing solutions by limitation of the sliding conditions, by using an observer, etc. In this section, we shall describe techniques for limitation of the sliding condition, as they are the most often used for applications in real time. Such techniques are based on definition of a zone around surface S within which a sliding condition less strict than the sign condition is applied. Thus, the term sgn (S) in the sliding part of the control is often replaced by a term with lighter variation, such as integral control or control with a threshold [10].

6.2 Advantage of Backstepping Control

One major advantage of Backstepping control is that nonlinearities can be treated in several ways, with useful nonlinearities contributing to stabilization retained in the Lyapunov function and non-useful nonlinearities replaced by linear control, requiring a control effort and, better yet, optimal resulting control laws guaranteeing a degree of robustness [11].

7 Conclusion

This work describes various control strategies applied to wind energy conversion systems (WECSs) based on DFIGs. We have designed and compared two control strategies for the grid-side converter (GSC): nonlinear backstepping control and sliding mode control.

To the diversity of methods for analysis of nonlinear systems, there is a corresponding diversity of design methods. Depending on the importance of the nonlinear phenomenon present in the system, these methods provide necessary and adequate conditions for good functioning.

Through response characteristics, we observe good performances even in the presence of instruction variations.

Pursuit of power is assured as is decoupling, stability and convergence towards balance. Furthermore, such regulation presents a very simple and robust algorithm control, which has the advantage of being easily integrated into computer control.

As presented, the backstepping method assumes availability of measurement of the state of the whole process. When a part of such state is not measurable, backstepping cannot be applied. A solution then consists of replace the state by an estimation made by an observer.

References

1. Lazhar, R.: Modélisation et Commande de la Génératrice à Induction Double Alimentée Couplée sur un Réseau Electrique (2012)
2. Gaillard, A.: Docteur de l'Université Henri Poincaré, Nancy-I
3. Poitiers, F.: Etude et commande de generatrices asynchrones pour l'utilisation de l'energie eolienne-Machine asynchrone à cage autonome-Machine asynchrone à double alimentation reliée au réseau, Université de Nantes (2003)
4. Multon, B., Roboam, X., et al.: Aérogénérateurs électriques (2006)
5. Ghennam, T., Berkouk, E.M., François, B., et al.: Modeling and Control of a Doubly Fed Induction Generator (DFIG) Based Wind Conversion System (2009)
6. Cherif, B.: Simulation de la commande vectorielle par régulateurs à mode glissant d'une chaîne éolienne à base d'une machine asynchrone à double alimentation (2014)
7. Errami, Y., Ouassaid, M., Maaroufi, M., et al.: A performance comparison of a nonlinear and a linear control for grid connected PMSG wind energy conversion system. Int. J. Electr. Power Energy Syst. **68**, 180–194 (2015)
8. Guessas, M.L.: Backstepping Backstepping adaptatif pour le contrôle la poursuite et la synchronisation des systèmes dynamiques non linéaires chaotiques, Université de Biskra (2012)
9. Khedher, A., Khemiri, N., Mimouni, M.F., et al.: Wind Energy Conversion System Using DFIG Controlled by Backstepping and Sliding Mode Strategies. Int. J. Renew. Energy Res. IJRER **2**(3), 421–430 (2012)
10. El Mahdi, A.S.A.: Commande en vitesse par mode glissant d'une Machine Asynchrone à Double Alimentation
11. Benaskeur, A.R.: Aspects de l'application du backstepping adaptatif à la commande décentralisée des systèmes non linéaires (2000)